

# An MO study of regioselective amine addition to *ortho*-quinones relevant to melanogenesis

 Edward J. Land,<sup>a</sup> Christopher A. Ramsden<sup>a,\*</sup> and Patrick A. Riley<sup>b</sup>
<sup>a</sup>Lennard-Jones Laboratories, School of Physical and Geographical Sciences, Keele University, Keele, Staffordshire ST5 5BG, UK

<sup>b</sup>Totteridge Institute for Advanced Studies, The Grange, Grange Avenue, London N20 8AB, UK

Received 8 December 2005; revised 17 February 2006; accepted 2 March 2006

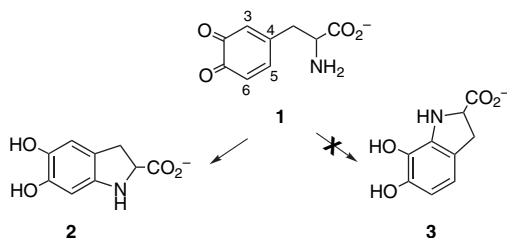
Available online 31 March 2006

**Abstract**—Energy profiles for alternative intramolecular cyclisations of 4-(aminoalkyl)-*ortho*-quinones have been calculated using the AM1 method and ab initio energies of the transition states are determined. In all the cases cyclisation at position 5 occurs via a significantly lower energy transition state than cyclisation at position 3. This is consistent with experimental observations. Optimal trajectories for attack have been determined from a study of the reactions of methylamine with 4-methyl-*ortho*-quinone. For cyclisation of aminoalkyl derivatives deviation from the optimal direction is less for reaction at position 5 but constraint on angle of attack only partially accounts for the regioselectivity. Intrinsic differences in the electronic energies of the alternative transition states are the main contributor to regioselectivity. The relative energies of transition states can be modified by variation of the substituent at position 4. The calculations suggest that seven-membered ring formation may occur via a boat transition state and steric hindrance in the seven-membered transition states may account for the experimentally observed influence of *N*-substituents on the mode of reaction.

© 2006 Elsevier Ltd. All rights reserved.

## 1. Introduction

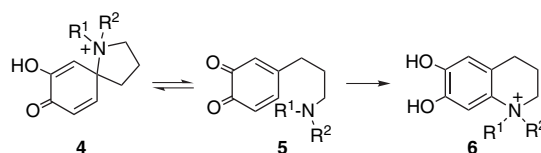
An important early step in the biosynthesis of eumelanin (a black-brown pigment) is the intramolecular cyclisation of dopaquinone **1** to cyclodopa **2**.<sup>1–3</sup> No evidence of the alternative cyclisation mode (**1** → **3**) (Scheme 1) has been observed.



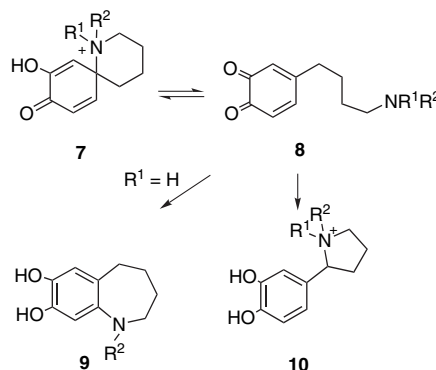
Scheme 1.

We have studied a number of analogues of dopaquinone **1**, including higher homologues, using NMR, tyrosinase oximetry and pulse radiolysis.<sup>4–9</sup> In none of our studies have we observed evidence of the alternative cyclisation at position 3. Increasing the chain length still results in exclusive cyclisation at position 5, although for propyl- and butylamines **5** and **8** (Schemes 2 and 3) we have observed that the spiro derivatives **4** and **7**, resulting from attack at position 4, are the kinetic products and these rapidly equilibrate to the

thermodynamic products **6** and **9**. Recently we have isolated a stable spirocyclic product.<sup>5</sup> In the case of the *n*-butyl tertiary amines **8** ( $R^1 \neq H$ ,  $R^2 \neq H$ ) cyclisation is not observed and much slower formation of the isomeric *para*-quinomethane occurs leading to the product **10**. Other modifications of the side chain (Eqs. 1<sup>5</sup> and 2<sup>9</sup>) similarly give exclusively the product from cyclisation at position 5.



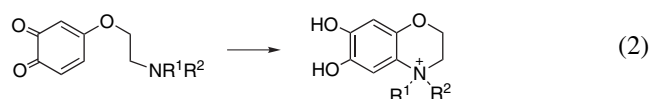
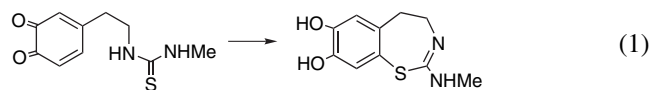
Scheme 2.



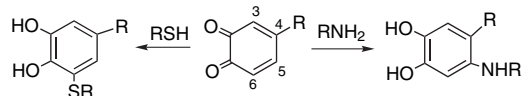
Scheme 3.

\* Corresponding author. Tel.: +44 178 258 3045; fax: +44 178 271 2378; e-mail: c.a.ramsden@chem.keele.ac.uk

The regioselectivity of these intramolecular cyclisations is consistent with the intermolecular reactions of *ortho*-quinones with amines and other nucleophiles, which usually give Michael addition products at position 5.<sup>10</sup> This is in interesting contrast with the reactions of *ortho*-quinones with thiols (RSH), which even under basic conditions (RS<sup>-</sup>), give exclusively or mainly the 6-addition products (Scheme 4).<sup>11–13</sup> This mode of reaction with cysteine is an early step in the formation of pheomelanin (a red-yellow pigment).<sup>3</sup>



In addition to being relevant to the biosynthesis of eumelanin and pheomelanin, the formation of endogenous *ortho*-quinones may be associated with the initiation of some cancers by reaction with DNA-amines or glutathione.<sup>14,15</sup> The mechanisms of these reactions are also of fundamental chemical interest. To explore the origins of the selectivity in these quinone reactions, we have carried out molecular orbital studies. In this paper we report the results for inter- and intramolecular reactions of *ortho*-quinones with primary amines.



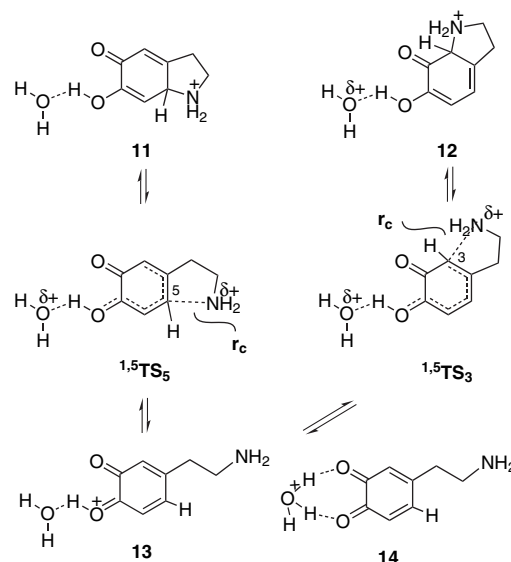
Scheme 4.

## 2. Results and discussion

### 2.1. 1,5-Intramolecular cyclisation and intermolecular reactions

The retro-1,5-cyclisations **11** → **13** and **12** → **13** (Scheme 5) were studied using the AM1 method by increasing the appropriate C–N interatomic distance ( $r_c$ ) in increments of ca. 0.05–0.1 Å. For each value of the reaction coordinate ( $r_c$ ) the energy was minimised with respect to all other variables. In the following discussion, for intramolecular cyclisations the size of the ring forming in the transition state (TS) is designated by a superscript and the ring position of the reaction by a subscript (e.g., <sup>1,5</sup>TS<sub>5</sub>). To allow for the role of proton transfer during quinone amine cyclisation in vivo, leading to intermediate enols (e.g., **11** and **12**), a hydrogen bonded water molecule was included in the calculations. In fact the calculated retro-reactions (Scheme 5) led to a protonated *ortho*-quinone **13**, rather than a hydrogen bonded quinone. However, the hydrogen bonded quinone **14** ( $\Delta H_f$  70.54 kcal mol<sup>-1</sup>) was calculated to be only 1.2 kcal mol<sup>-1</sup> higher in energy than the protonated quinone **13** ( $\Delta H_f$  69.36 kcal mol<sup>-1</sup>). Since this study is primarily concerned with the relative energies of similar alternative transition states formed from common precursors (e.g., **13** or **14**) the exact nature of the solvation of the precursor amines is not

an essential requirement. It is beyond the scope of this study to investigate accurate absolute energies of the species involved.



Scheme 5.

The AM1 energy profiles for the alternative reaction pathways to positions 5 and 3 via the transition states <sup>1,5</sup>TS<sub>5</sub> and <sup>1,5</sup>TS<sub>3</sub> are shown in Figure 1. In agreement with experimental observations it can be seen that cyclisation at the 5-position is favoured. For both the cyclisations the transition state is calculated to occur at a C–N separation of ca. 2.2 Å. To obtain a more accurate estimate of the relative transition state energies their electronic energies were determined by ab initio calculations at the RHF/6-31G\*\* level using the AM1 geometries. The results of these calculations and the relative energies of transition states are summarised in

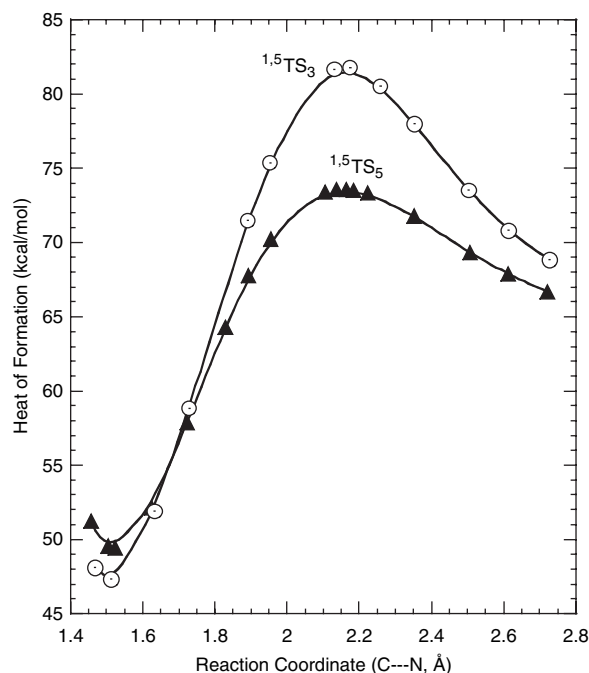


Figure 1. AM1 energy profiles for cyclisation of 4-(2-aminoethyl)-*ortho*-quinone at positions 3 (O) and 5 (▲) (Scheme 5).

**Table 1.** Ab initio electronic energies (au) and relative energies (kcal mol<sup>-1</sup>) for transition states

Reaction mode	Transition state (TS)	RHF/6-31G** (a.u.)	Rel energy (kcal mol <sup>-1</sup> ) <sup>a</sup>
Intermolecular	TS <sub>3</sub>	-589.58129	12.1 (6.3)
	TS <sub>5</sub>	-589.60063	0.0 (0.0)
	TS <sub>6</sub>	-589.59264	5.0 (2.6)
1,5-Intramolecular	<sup>1,5</sup> TS <sub>3</sub>	-588.40625	17.7 (8.2)
	<sup>1,5</sup> TS <sub>5</sub>	-588.43439	0.0 (0.0)
1,6-Intramolecular	<sup>1,6</sup> TS <sub>3</sub> (chair)	-627.43690	15.9 (7.4)
	<sup>1,6</sup> TS <sub>3</sub> (twist boat)	-627.43210	18.9 (8.3)
	<sup>1,6</sup> TS <sub>5</sub> (chair)	-627.46217	0.0 (0.0)
	<sup>1,6</sup> TS <sub>5</sub> (twist boat)	-627.45742	3.0 (1.2)
1,7-Intramolecular	<sup>1,7</sup> TS <sub>3</sub> (chair)	-666.44647	14.1 (5.9)
	<sup>1,7</sup> TS <sub>3</sub> (boat)	-666.45430	9.2 (6.0)
	<sup>1,7</sup> TS <sub>5</sub> (chair)	-666.46891	0.0 (0.0)
	<sup>1,7</sup> TS <sub>5</sub> (boat)	-666.47077	-1.2 (0.0 <sub>5</sub> )

<sup>a</sup> Defined with respect to the lowest energy AM1 transition state for the reactant(s); values in brackets are for the AM1 calculations.

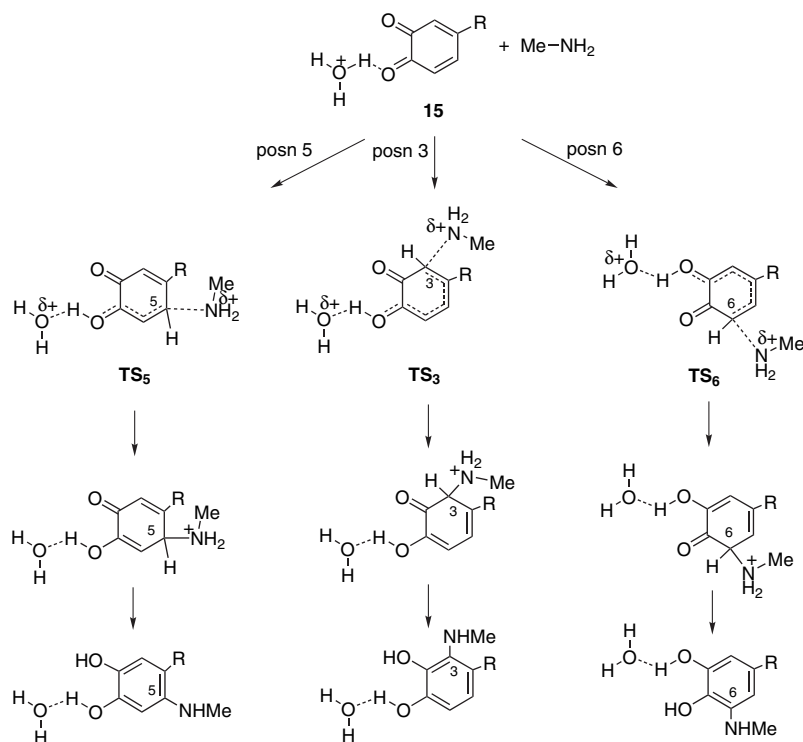
**Table 1.** It can be seen that the ab initio method suggests an even greater energy difference (17.7 kcal mol<sup>-1</sup>) between transition states <sup>1,5</sup>TS<sub>5</sub> and <sup>1,5</sup>TS<sub>3</sub> than the AM1 method (8.2 kcal mol<sup>-1</sup>) and the results are entirely consistent with the observed regioselectivity.

Based on these calculations there is a significant energetic preference for cyclisation at the 5-position of the ring. At this stage it was not clear whether this energy difference arises from constraints on the angle at which the amine can approach the sp<sup>2</sup> carbon atom or inherent electronic energy differences in the isomeric transition states. To determine the optimum angle of approach for each ring position and the relative energies of unrestricted acyclic transition states we calculated the energy profiles of the reactions of

methylamine at positions 3, 5 and 6 of 4-methyl-*ortho*-quinone **15** (R=Me) (Scheme 6). Again the retro-reactions were studied using the appropriate C–N separation as reaction coordinate and increasing this parameter by increments of ca. 0.05–0.1 Å. For reaction at positions 3 and 6, after the transition state had been passed in the retro-reactions there was a tendency for the nitrogen to attack the neighbouring carbonyl group. This is consistent with experimental observation (see below). To prevent this, for  $r_c > 2.25$  Å the angle N–C3–C2 (or N–C6–C1) was restricted to that at the transition state (92°). Otherwise, all variables except the reaction coordinate were minimised.

The results of these AM1 calculations are shown in Figure 2. Single-point ab initio energies were calculated for the transition states (Table 1). As for the 1,5-intramolecular cyclisation reactions, reaction at the 5-position is calculated to be energetically preferred over reaction at the 3-position by 6.3 kcal mol<sup>-1</sup> (AM1) and 12.1 kcal mol<sup>-1</sup> (ab initio). The transition state for reaction at position 6 is intermediate in energy. We observed that there is a shallow energy minimum at C5–N 2.75 Å (Fig. 2), which is presumably due to a weak favourable interaction between the quinone and the amine. These calculations are in agreement with experimental observations in which reactions of *ortho*-quinones with amines are found to occur by conjugate addition at position 5.<sup>16–18</sup> If this mode of reaction is prevented by substituents or steric hindrance then nucleophilic attack at one of the carbonyl carbons occurs.<sup>19</sup>

We assume that the calculated angles of approach are optimal for the intermolecular methylamine reactions for which there are no constraints at the transition state. These optimal angles (see Fig. 3) are: (i) for attack at C5: N–C5–C6=99.7°,

**Scheme 6.**

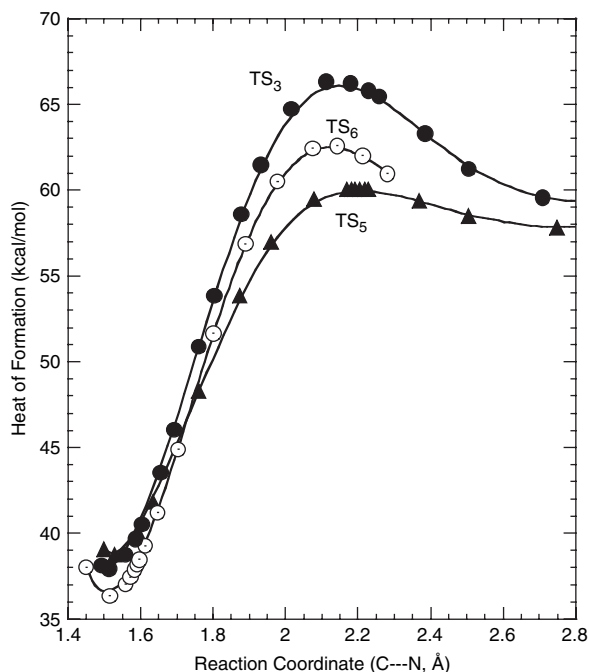


**Figure 2.** AM1 energy profiles for reaction of methylamine with 4-methyl-*ortho*-quinone at positions 3 (●), 5 (▲) and 6 (○) (Scheme 6).

N–C5–C4=97.3° and (ii) for attack at C3: N–C3–C4=102.8°, N–C3–C2=94.2°.

It is instructive to compare these with the corresponding angles of approach in the constrained intramolecular reactions (Scheme 5). The optimal directions of approach were defined relative to atoms C4,C5,C6 (attack at C5) or C2,C3,C4 (attack at C3) using the angles determined above for the intermolecular reactions of methylamine. The deviations from the optimal direction in transition state  $^{1,5}\text{TS}_5$  can then be estimated in terms of the angular deviation ( $\Phi$ ) from the optimal direction and the orientation of this deviation ( $\vartheta$ ) relative to the C5–C6 bond as shown in Figure 3a. Similar parameters ( $\Psi$  and  $\pi$ ) can be defined with respect to the C3–C4 bond for cyclisation at position 3 (Fig. 3b).

Using this approach we calculated the following deviations from optimal nucleophilic attack for the 2-aminoethyl side chain: (i) cyclisation at position 5 (i.e.,  $^{1,5}\text{TS}_5$ ) [ $\Phi=11.8^\circ$  and  $\nu=198^\circ$ ] and (ii) cyclisation at position 3 (i.e.,  $^{1,5}\text{TS}_3$ ) [ $\Psi=17.9^\circ$  and  $\pi=46^\circ$ ]. It can be seen that neither mode of 1,5-intramolecular cyclisation permits the optimum direction of nucleophilic attack but the observed cyclisation at position 5 is closest ( $\Phi=12^\circ$  vs  $\Psi=18^\circ$ ) (see also Table 2).

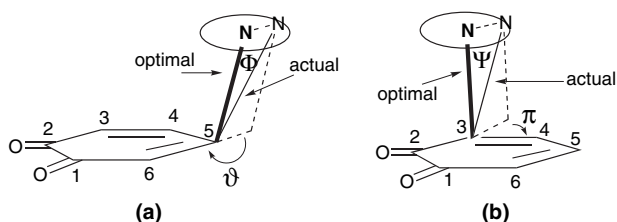


**Figure 3.** Definition of optimal and actual directions for intramolecular nucleophilic attack by amines at (a) position 5 and (b) position 3.

**Table 2.** Calculated angles of nucleophilic attack at transition states relative to optimal angle (Fig. 3)

Reaction mode	Transition state (TS)	Position 5		Position 3	
		$\Phi$	$\vartheta$	$\Psi$	$\pi$
Intermolecular	—	0°	0°	0°	0°
1,5-Intramolecular	—	12°	198°	18°	46°
1,6-Intramolecular	Chair	5°	209°	6°	14°
	Twist boat	4°	219°	5°	4°
1,7-Intramolecular	Chair	4°	265°	6°	306°
	Boat	2°	262°	1°	342°

Figure 4 shows the calculated structures of the  $^{1,5}\text{TS}_5$  and  $^{1,5}\text{TS}_3$  transition states together with the optimal direction of approach, estimated from the reaction with methylamine, indicated by the yellow dummy atom.

To determine the influence of distorting the direction of nucleophilic attack away from the optimal direction on transition state energy we investigated the effect of constraining the transition states for the intermolecular methylamine reactions to the corresponding 1,5-intramolecular trajectories. For attack at position 5 angles N–C5–C6 and N–C5–C4 were fixed at the values in  $^{1,5}\text{TS}_5$  (i.e., N–C5–C6=110° and N–C5–C4=88°). All parameters other than C5–N (2.2 Å) were allowed to relax. This distortion resulted in an AM1 calculated heat of formation of the transition state of 71.3 kcal mol<sup>-1</sup>, which is an increase of 11.2 kcal mol<sup>-1</sup> over the optimal transition state energy. Clearly, deviation of 12° (Fig. 3) from the optimal trajectory causes a significant increase in energy. A similar AM1 calculation for attack at position 3 using the angles for  $^{1,5}\text{TS}_3$  (N–C3–C4=90° and N–C3–C2=110°) resulted in an increase of transition state energy of 14.2 kcal mol<sup>-1</sup>. The difference in the AM1 energies of the distorted transition states (9.2 kcal mol<sup>-1</sup>) is comparable to the energy difference between the cyclic transition states  $^{1,5}\text{TS}_5$  and  $^{1,5}\text{TS}_3$  (8.2 kcal mol<sup>-1</sup>). This suggests that the distortion from the ideal angles (for which the energy difference is 6.3 kcal mol<sup>-1</sup>) contributes ca. 2–3 kcal mol<sup>-1</sup> to the total AM1 energy difference between the transition states (8.2 kcal mol<sup>-1</sup>). Ab initio calculations on the same distorted acyclic transition states suggest that distortion contributes ca. 6–9 kcal mol<sup>-1</sup> to the calculated energy difference of 17.7 kcal mol<sup>-1</sup> between  $^{1,5}\text{TS}_5$  and  $^{1,5}\text{TS}_3$ . Based on these estimates, there is clearly a positive correlation between an increase in  $\Phi$  or  $\Psi$  and increase in transition

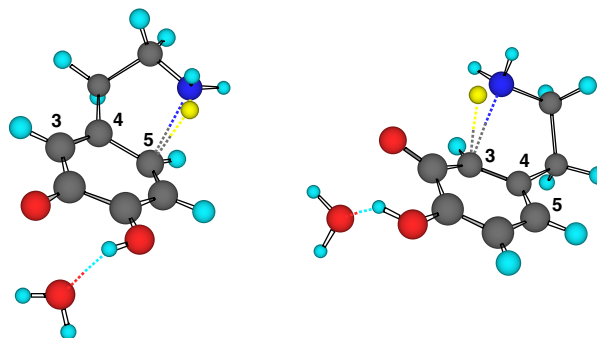


**Figure 4.** Calculated transition states  $^{1,5}\text{TS}_5$  and  $^{1,5}\text{TS}_3$  including optimal angles for nucleophilic attack (yellow atoms) estimated from intermolecular reaction of MeNH<sub>2</sub>.

state energy, and this effect can be expected to favour intramolecular nucleophilic attack at position 5. This may partly explain why intramolecular attack at position 5 is preferred but clearly it is not the only effect favouring reaction at position 5.

Even when there is no constraint on angle of approach, as in the methylamine–4-methylquinone reaction (Scheme 6; R=Me), there is a clear preference for nucleophilic attack at position 5 (Fig. 2). We conclude, therefore, that the main source of the energetic preference for attack at position 5 is the intrinsic difference in the electronic energies of the two similar but different transition states (**TS<sub>5</sub>** vs **TS<sub>3</sub>**) (Scheme 6). In the preferred mode of reaction (**TS<sub>5</sub>**) one  $\alpha,\beta$ -unsaturated ketone function remains unperturbed during reaction whereas in the alternative mode (**TS<sub>3</sub>**) both the formal C–C double bonds of the quinone are broken to form the transition state (Scheme 6).

It is of interest to investigate the influence of the substituent R on the relative energies of the transition states **TS<sub>5</sub>** and **TS<sub>3</sub>** (Scheme 6). Assuming that the transition states occur at the same C–N separation (2.2 Å), we have investigated the relative energies for nine substituents (R) for which there is a wide variation in electronic properties. Apart from the reaction coordinate all structural parameters were optimised for each transition state and the results are summarised in Table 3, together with the corresponding Swain and Lupton electronic parameters ( $\mathcal{F}$ ,  $\mathcal{R}$  and  $\mathcal{R}^+$ ).<sup>20</sup>

$$\Delta H_f[\text{TS}_3 - \text{TS}_5] = 4.000 - 5.646 \mathcal{R}^+ \quad n=9, r=0.959 \quad (3)$$

$$\Delta H_f[\text{TS}_3 - \text{TS}_6] = 0.611 - 11.376 \mathcal{R}^+ \quad n=9, r=0.950 \quad (4)$$

From Table 3 it can be seen that even in the absence of a substituent (R=H) attack at position 5 is favoured over position 3 by ca. 5 kcal mol<sup>-1</sup>, as measured by the calculated difference in transition state energies ( $\Delta H_f[\text{TS}_3 - \text{TS}_5]$ ). In general, reaction at position 5 becomes increasingly favoured as the negative resonance effect of the substituent R increases (i.e., Swain and Lupton resonance constant  $\mathcal{R}$  negative). This can be interpreted as a favourable resonance/hyperconjugation interaction between substituent R and the  $\alpha,\beta$ -unsaturated ketone fragment that is retained throughout the reaction at position 5 but which is lost (or

less favourable) when reaction occurs at position 3. In contrast, when the substituent R has a positive resonance effect (i.e., CF<sub>3</sub> and CN) resonance favours the alternative transition state (**TS<sub>3</sub>**) but the effect is not large enough to reverse the preferred mode of reaction. In this context it is instructive to consider the transition state for reaction at position 3 in terms of partial formation of a dienolate anion (cf. **16** and **17**). In this mode of reaction (**TS<sub>3</sub>**) negative charge can be expected to develop at position 4 (and 6) and this can be expected to be stabilised by substituents with a positive resonance effect (i.e., CF<sub>3</sub> and CN). In contrast, substituents with a negative resonance effect will not favour **TS<sub>3</sub>**, while at the same time favouring **TS<sub>5</sub>**. A good correlation between  $\mathcal{R}$  and  $\Delta H_f[\text{TS}_3 - \text{TS}_5]$  was found and this was improved using the cationic constant  $\mathcal{R}^+$  (Eq. 3) ( $\sigma^+ = \mathcal{F} + \mathcal{R}^+$ ). Use of  $\mathcal{R}^+$  does not seem unreasonable as *ortho*-quinones are electron deficient species.

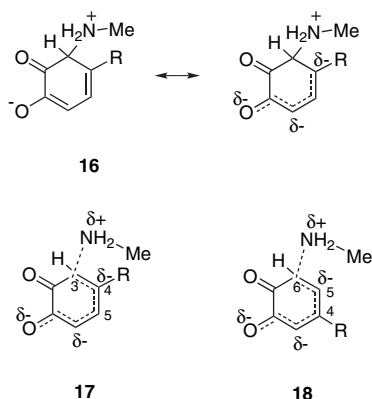
This interpretation of the substituent effect at position 4 is reinforced by considering the influence of substituents on competition between nucleophilic attack at positions 3 and 6 (i.e., **17** vs **18**). In this case the transition states (**TS<sub>3</sub>** and **TS<sub>6</sub>**) are identical when R=H. Any difference when R is varied is therefore entirely due to the nature of the substituent. Table 3 shows the calculated differences in transition state energies ( $\Delta H_f[\text{TS}_3 - \text{TS}_6]$ ) for the same set of substituents. As might be expected by considering the structures **17** and **18**, substituents R with a negative resonance effect (e.g., Me, OMe) favour transition state **TS<sub>6</sub>** and those with a positive resonance effect (e.g., CF<sub>3</sub>, CN) favour transition state **TS<sub>3</sub>**. However, in all cases **TS<sub>5</sub>** is still the energetically favoured mode of reaction. There is a good correlation between the difference in calculated transition state energy  $\Delta H_f[\text{TS}_3 - \text{TS}_6]$  and  $\mathcal{R}$ , and this correlation is improved using  $\mathcal{R}^+$  (Eq. 4).

We conclude that for 1,5-cyclisation of 4-(2-aminoethyl)-*ortho*-quinones the intrinsic difference in electronic energy of the alternative transition states favours cyclisation at position 5. The energy advantage of cyclisation at position 5 may be related to the fact that during this mode of reaction an  $\alpha,\beta$ -unsaturated ketone function remains unperturbed. In addition, the alkyl chain at position 4 probably increases the preference for position 5 due to a negative resonance effect. This mode of reaction is also enhanced by the more favourable trajectory of approach to the ring carbon atom compared to reaction at position 3.

**Table 3.** AM1 calculated transition state energies for a series of 4-substituted *ortho*-quinones reacting with methylamine

R	$\Delta H_f[\text{TS}_5]$	$\Delta H_f[\text{TS}_3]$	$\Delta H_f[\text{TS}_6]$	$\Delta H_f[\text{TS}_3 - \text{TS}_5]$	$\Delta H_f[\text{TS}_3 - \text{TS}_6]$	$\mathcal{F}$	$\mathcal{R}$	$\mathcal{R}^+$
H	69.2	74.1	74.1	4.9	0	0	0	0
Me	60.1	66.3	62.6	6.2	3.7	-0.04	-0.13	-0.27
Cl	65.7	71.1	68.6	5.4	2.5	0.41	-0.15	-0.30
OH	23.9	33.8	22.1	9.9	11.7	0.29	-0.64	-1.21
CF <sub>3</sub>	-78.5	-76.4	-69.9	2.1	-6.5	0.38	0.19	0.23
SH	72.1	80.3	68.6	8.2	10.7	0.28	-0.11	(-1) <sup>a</sup>
OMe	27.9	38.2	25.9	10.3	12.3	0.26	-0.51	-1.04
SMe	64.4	73.7	60.7	9.3	13.0	0.20	-0.18	-0.74
CN	108.8	112.1	114.1	3.3	-0.2	0.51	0.19	0.15

<sup>a</sup> Estimated.



## 2.2. 1,6-Intramolecular cyclisation

Cyclisation of the 3-aminopropyl derivative **19** to positions 3 or 5 leading to the intermediates **20** or **21** (Scheme 7) was modelled as described for the 2-aminoethyl derivative. In this case two alternative transition states were found for each position of reaction. For both the pathways the lower energy transition state has a chair conformation and the higher energy transition state had a twist boat conformation. However, in each case the twist boat structure is only ca. 1 kcal mol<sup>-1</sup> higher in energy than the chair structure and these alternative conformations are not relevant to the preferred mode of cyclisation. As for the 2-aminoethyl derivative, cyclisation at position 5 is calculated to be kinetically favoured. The calculated energy profiles are shown in Figure 5. The difference in heats of formation of the alternative chair transition states <sup>1,6</sup>TS<sub>5</sub> and <sup>1,6</sup>TS<sub>3</sub> are 7.4 kcal mol<sup>-1</sup> (AM1) and 15.9 kcal mol<sup>-1</sup> (ab initio) (Table 1). The calculated angles of approach relative to the optimum, as defined in Figure 3, for all four transition states are shown in Table 2. For these cyclisations the deviations from optimal ( $\Phi, \Psi \approx 4-6^\circ$ ) are much smaller than for the five-membered transition states and there is no significant difference between reaction at position 3 and position 5. This effect may marginally favour reaction at position 5 but it is small. The factors that favour reaction at position 5 are probably essentially those that favour similar attack in the intermolecular methylamine reaction discussed above.

## 2.3. 1,7-Intramolecular cyclisation

Finally we have calculated the cyclisation pathway for the 4-aminobutyl side chain **22**. As for the 3-aminopropyl cyclisa-

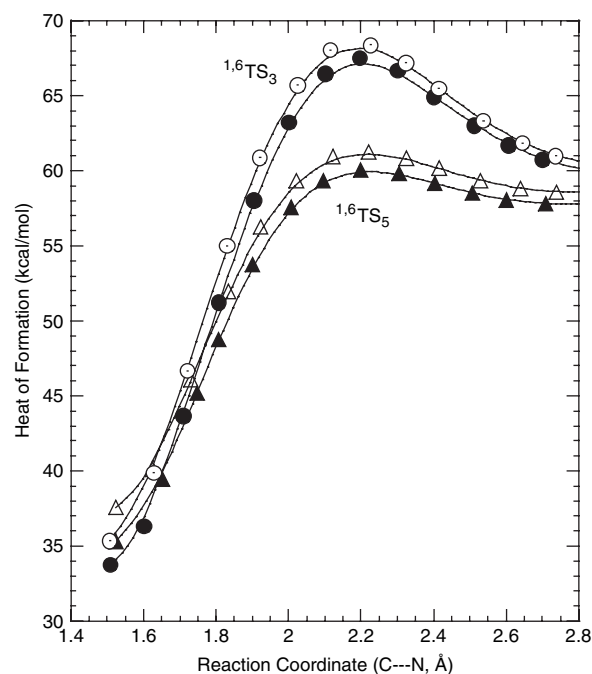
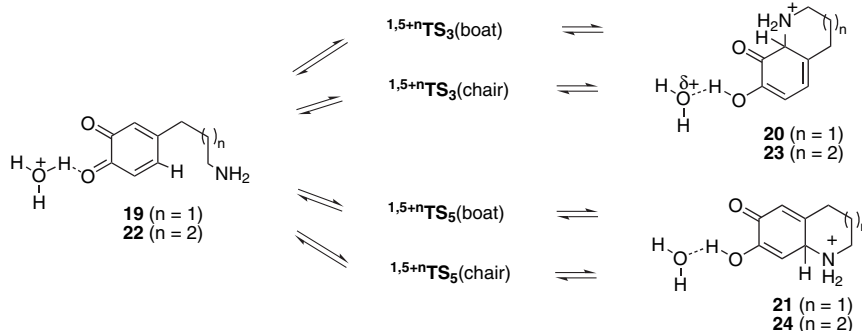


**Figure 5.** AM1 energy profiles for cyclisation of 4-(3-aminopropyl)-ortho-quinone at positions 3 (●, chair; ○, twist boat) and 5 (▲, chair; △, twist boat) (Scheme 7).

tions, each mode of ring-closure can occur via a chair or boat transition state (Fig. 6), with each pair being close in energy (Scheme 7). As previously, the cyclisation at position 5 is calculated to be energetically preferred with a difference in calculated heats of formation between <sup>1,7</sup>TS<sub>5</sub> and <sup>1,7</sup>TS<sub>3</sub> of 5.9 kcal mol<sup>-1</sup> (AM1) and 10.4 kcal mol<sup>-1</sup> (ab initio) (Table 1). For all four modes of reaction deviation from the optimal angle of approach is small (Table 2). It is significant to note that at the RHF/6-31G\*\* level the boat transition states are calculated to be more stable than the chair transition states (Table 1) and for <sup>1,7</sup>TS<sub>5</sub> (boat) the angle of approach deviates only 1° from the optimal angle (Table 2). It is therefore possible that these cyclisations occur, at least partially, via the boat transition states (Fig. 6b).

A feature of the transition states for reaction at position 5 is the close approach of the protons on C5 and C3' for <sup>1,7</sup>TS<sub>5</sub> (chair) (2.19 Å) and on C5 and C2' for <sup>1,7</sup>TS<sub>5</sub> (boat) (2.08 Å) (Fig. 6). Similar close interactions do not arise in the transition states for shorter chains, and these interactions in the seven-membered transition states may be the primary



**Scheme 7.**

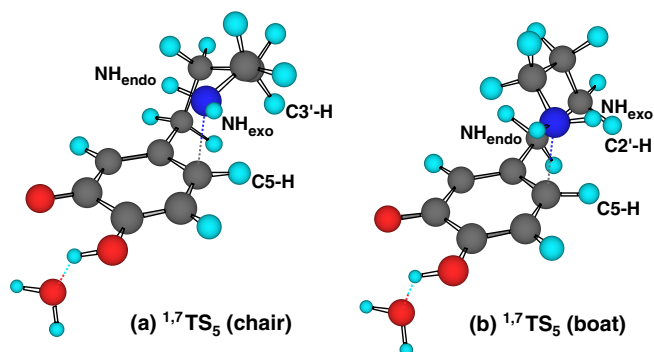


Figure 6. Calculated  $^{1,7}\text{TS}_5$  chair and boat transition states.

source of substituent effects that we have observed experimentally.<sup>6,21</sup> In particular, we have observed that tertiary amine derivatives ( $-\text{NR}_2$ ) do not cyclise at either position 5 or 3. Instead quinomethane formation occurs via a pathway that is normally much slower (Scheme 3; **8**  $\rightarrow$  **10**). Significantly, calculations on the *N,N*-dimethyl, *N,N*-diethyl and *N,N*-di-*n*-propyl chair transition states showed that the C5-H, C3'-H separation decreased to 2.09 Å (and for the boat transition states the C5-H, C2'-H separation decreased to 2.00 Å). In contrast to tertiary amines, simple secondary amines ( $-\text{NHR}$ , R=alkyl) do cyclise via a  $^{1,7}\text{TS}_5$  transition state and calculations on the NHMe (*exo*) and NHPPr (*exo*) derivatives gave increased chair C5-H, C3'-H separations of 2.17 and 2.18 Å. Similarly, the NHMe (*endo*) and NHPPr

(*endo*) derivatives gave increased boat C5-H, C2'-H separations of 2.08 and 2.06 Å. We have observed that the NH<sup>*t*</sup>Bu derivative also does not readily cyclise and behaves like a tertiary amine leading to quinomethane formation.<sup>6,21</sup> A calculation of this amine showed the C5-H, C3'-H separation to be 2.07 Å, together with other unfavourable H-H interactions ( $<2.1$  Å) due to the methyl substituents. Significantly, the NH<sup>*t*</sup>Pr derivative does cyclise<sup>6,21</sup> and a calculation showed that this amine can adopt a conformation in the  $^{1,7}\text{TS}_5$  chair transition state, in which the <sup>*t*</sup>Pr C-H bond is *anti* to the N-C4' bond, such that the C5-H, C3'-H separation is 2.18 Å.

It therefore appears that an adverse C5-H, C2'- or C3'-H interaction in the transition state is a significant factor in inhibiting  $^{1,7}\text{TS}_5$  cyclisation and that derivatives, which do not cyclise in experimental studies<sup>6,21</sup> have AM1 calculated separations that are less than those that do cyclise. The results are summarised in Table 4. We believe that these subtle steric interactions in the transition states inhibit 1,7-cyclisation of tertiary amines and *N-t*-butyl derivatives allowing slower alternative reactions to occur (Scheme 3).

### 3. Conclusions

Our calculations show that for both inter- and intramolecular additions of amines to *ortho*-quinones reaction at position 5 of the ring is favoured over reaction at position 3. The calculated heats of formation of all reactants, products and transition states are summarised in Table 5. Although we have previously noted that there is a shallow energy minimum at  $r_c \sim 2.75$  Å, to avoid ambiguity the heats of formation of the reactants shown in Table 5 are calculated for maximum separation of ring and amine or, for intermolecular reactions, a separation of 10 Å.

The calculations suggest that reaction at position 5 is favoured due to the intrinsically lower electronic energy of the ' $\text{TS}_5$ ' transition states in which an  $\alpha,\beta$ -unsaturated ketone function remains unperturbed throughout the reaction. The energy difference can be modified by the nature of the substituent at position 4 but no substituent effects are large enough to reverse the regioselectivity. A secondary factor is the trajectory of the incoming amine and for five-member ring formation, which is particularly relevant to melano-genesis (Scheme 1), this also favours reaction at position 5.

Table 4. Calculated close H-H interactions for  $^{1,7}\text{TS}_5$  transition states

Nucleophile NR <sub>2</sub>	$^{1,7}\text{TS}_5$ (chair)	$^{1,7}\text{TS}_5$ (boat)
	C5-H-C3'-H (Å)	C5-H-C2'-H (Å)
NH <sub>2</sub>	2.19	2.08
NMe <sub>2</sub>	2.09	2.00
NEt <sub>2</sub>	2.09	2.01
N <sup><i>n</i></sup> Pr <sub>2</sub> <sup>a</sup>	2.09	2.01
NHMe ( <i>exo</i> )	2.17	2.03
NHMe ( <i>endo</i> )	2.12	2.08
NH <sup><i>n</i></sup> Pr ( <i>exo</i> ) <sup>b</sup>	2.18	2.05
NH <sup><i>n</i></sup> Pr ( <i>endo</i> ) <sup>b</sup>	2.11	2.06
NH <sup><i>t</i></sup> Pr ( <i>exo</i> ) <sup>b</sup>	2.18	2.07
NH <sup><i>t</i></sup> Bu ( <i>exo</i> ) <sup>a</sup>	2.07	2.03

<sup>a</sup> These groups do not undergo 1,7-cyclisation in experimental studies.<sup>6,21</sup>

<sup>b</sup> These groups have been shown experimentally to undergo 1,7-cyclisation.<sup>6,21</sup>

Table 5. AM1 stationary point energies for *ortho*-quinone-amine reactions

Reaction mode	Transition state (TS)	Reactant(s) $\Delta H_f$ [R]	Product $\Delta H_f$ [P]	TS $\Delta H_f$ [TS]	$\Delta\Delta H_f$ [TS] - $\Delta H_f$ [R]
Intermolecular	TS <sub>3</sub>	62.16	37.99	66.34	4.18
	TS <sub>5</sub>	62.16	38.75	60.06	-2.10
	TS <sub>6</sub>	62.16	36.36	62.61	0.45
1,5-Intramolecular	$^{1,5}\text{TS}_3$	69.36	47.32	81.74	12.38
	$^{1,5}\text{TS}_5$	69.36	49.42	73.57	4.21
1,6-Intramolecular	$^{1,6}\text{TS}_3$ (chair)	61.97	33.75	67.50	5.53
	$^{1,6}\text{TS}_3$ (twist boat)	61.97	35.39	68.42	6.45
	$^{1,6}\text{TS}_5$ (chair)	61.97	35.31	60.08	-1.89
	$^{1,6}\text{TS}_5$ (twist boat)	61.97	37.56	61.26	-0.71
1,7-Intramolecular	$^{1,7}\text{TS}_3$ (chair)	55.35	30.66	60.62	5.27
	$^{1,7}\text{TS}_3$ (boat)	55.35	31.70	60.70	5.35
	$^{1,7}\text{TS}_5$ (chair)	55.35	30.91	54.75	-0.60
	$^{1,7}\text{TS}_5$ (boat)	55.35	32.79	54.81	-0.54

#### 4. Calculations

The MOPAC program within *CS CHEM3D Pro*<sup>®</sup> (CambridgeSoft Corporation, Cambridge MA, USA) was used for AM1 calculations,<sup>22</sup> and the GaussView 3.0 program (Gaussian, Inc, Pittsburgh PA, USA) for ab initio calculations.<sup>23</sup> Transition states were stationary points. For improved energies single-point RHF/6-31G\*\* calculations were performed on AM1 optimised geometries.

#### References and notes

1. D'Ischia, M.; Napolitano, A.; Pezzella, A.; Land, E. J.; Ramsden, C. A.; Riley, P. A. *Adv. Heterocycl. Chem.* **2005**, *89*, 1–63.
2. Land, E. J.; Ramsden, C. A.; Riley, P. A. *Methods Enzymol.* **2004**, *378A*, 88–109.
3. Prota, G. *Melanins and Melanogenesis*; Academic: San Diego, CA, 1992.
4. Land, E. J.; Ramsden, C. A.; Riley, P. A. *Acc. Chem. Res.* **2003**, *36*, 300–308.
5. Land, E. J.; Perona, A.; Ramsden, C. A.; Riley, P. A. *Org. Biomol. Chem.* **2005**, *3*, 2387–2388.
6. Land, E. J.; Ramsden, C. A.; Riley, P. A.; Yoganathan, G. *Org. Biomol. Chem.* **2003**, *1*, 3120–3124.
7. Clews, J.; Cooksey, C. J.; Garratt, P. J.; Land, E. J.; Ramsden, C. A.; Riley, P. A. *J. Chem. Soc., Perkin Trans. 1* **2000**, 4306–4315.
8. Cooksey, C. J.; Garratt, P. J.; Land, E. J.; Pavel, S.; Ramsden, C. A.; Riley, P. A.; Smit, N. P. M. *J. Biol. Chem.* **1997**, *272*, 26226–26235.
9. Penn, A.; Ramsden, C. A., unpublished work.
10. Finley, K. T. The Addition and Substitution Chemistry of Quinones. In *The Chemistry of the Quinonoid Compounds*; Patai, S., Ed.; Wiley: London, 1974; pp 877–1144.
11. Prota, G.; Scherillo, G.; Napolano, E.; Nicolaus, R. A. *Gazz. Chim. Ital.* **1967**, *97*, 1451–1478.
12. Ito, S.; Prota, G. *Experientia* **1977**, *33*, 1118–1119.
13. Prota, G.; Petrillo, O.; Santacroce, C.; Sica, D. *J. Heterocycl. Chem.* **1970**, *7*, 555–561.
14. Cavalieri, E. L.; Rogan, E. G.; Chakravarti, D. *Cell. Mol. Life Sci.* **2002**, *59*, 665–681.
15. Monks, T. J.; Lau, S. S. *Crit. Rev. Toxicol.* **1992**, *22*, 243–270.
16. Adams, R. N.; Hawley, M. D.; Feldberg, S. W. *J. Phys. Chem.* **1967**, *71*, 851–855.
17. Horspool, W. M.; Smith, P. I.; Tedder, J. M. *J. Chem. Soc. C* **1971**, 138.
18. Schill, G.; Logemann, E.; Dietrich, B.; Lower, H. *Synthesis* **1979**, 695–697.
19. Corey, E. J.; Achiwa, K. *J. Am. Chem. Soc.* **1969**, *91*, 1429–1432.
20. Hansch, C.; Leo, A. J. *Substituent Constants for Correlation Analysis in Chemistry and Biology*; Wiley: New York, NY, 1979.
21. Land, E. J.; Ramsden, C. A.; Riley, P. A.; Yoganathan, G. *Pigment Cell Res.* **2003**, *16*, 397–406.
22. Dewar, M. J. S.; Zoebisch, E. G.; Healy, E. F.; Stewart, J. J. P. *J. Am. Chem. Soc.* **1985**, *107*, 3902–3909.
23. Frisch, M. J.; Trucks, G. W.; Schlegel, H. B.; Scuseria, G. E.; Robb, M. A.; Cheeseman, J. R.; Montgomery, J. A., Jr.; Vreven, T.; Kudin, K. N.; Burant, J. C.; Millam, J. M.; Iyengar, S. S.; Tomasi, J.; Barone, V.; Mennucci, B.; Cossi, M.; Scalmani, G.; Rega, N.; Petersson, G. A.; Nakasuji, H.; Hada, M.; Ehara, M.; Toyota, K.; Fukuda, R.; Hasegawa, J.; Ishida, M.; Nakajima, T.; Honda, Y.; Kitao, O.; Nakai, H.; Klene, M.; Li, X.; Knox, J. E.; Hratchian, H. P.; Cross, J. B.; Adamo, C.; Jaramillo, J.; Gomperts, R.; Stratmann, R. E.; Yazyev, O.; Austin, A. J.; Cammi, R.; Pomelli, C.; Ochterski, J. W.; Ayala, P. Y.; Morokuma, K.; Voth, G. A.; Salvador, P.; Dannenberg, J. J.; Zakrzewski, V. G.; Dapprich, S.; Daniels, A. D.; Strain, M. C.; Farkas, O.; Malick, D. K.; Rabuck, A. D.; Raghavachari, K.; Foresman, J. B.; Ortiz, J. V.; Cui, Q.; Baboul, A. G.; Clifford, S.; Cioslowski, J.; Stefanov, B. B.; Liu, G.; Liashenko, A.; Piskorz, P.; Komaromi, I.; Martin, R. L.; Fox, D. J.; Keith, T.; Al-Laham, M. A.; Peng, C. Y.; Nanayakkara, A.; Challacombe, M.; Gill, P. M. W.; Johnson, B.; Chen, W.; Wong, M. W.; Gonzalez, C.; Pople, J. A. *Gaussian 03, Revision B.01*; Gaussian: Pittsburgh, PA, 2003.